Proceedings of the 9th U.S. National and 10th Canadian Conference on Earthquake Engineering
Compte Rendu de la 9ième Conférence Nationale Américaine et
10ième Conférence Canadienne de Génie Parasismique
July 25-29, 2010, Toronto, Ontario, Canada • Paper No 1335

CAPACITY AND DEMAND EVALUATION OF MOMENT FRAMES WITH DIFFERENT HYSTERETIC BEHAVIOR

Z. Huang[1] and D. A. Foutch[2]

ABSTRACT

It is conjectured that different hysteresis behavior may lead to different levels of response because of degradation in strength and stiffness. To examine the existence and magnitude of this effect, this research aims to: 1. Determine the global collapse limits of several classes of moment frame buildings under seismic loads. 2. Develop bases for seismic criteria for design and evaluation of moment frame buildings that reflect and account for the global drift limit. 3. Evaluate the hysteresis effects on the demand level response and capacity/demand ratio of moment frame buildings under seismic loads. To achieve these objectives, seismic analyses of 3-, 9- and 20-story moment resisting frame buildings were conducted to evaluate the effects of the hysteretic behavior of beam-to-column connections on the collapse potential and the demand level response. Five hysteresis models: bilinear, strength degradation, stiffness degradation, stiffness degradation + strength degradation, and pinching are evaluated. The effects of hysteresis behaviors are very significant for both global drift limits and demand level responses. Two interesting results for the mid-rise/high-rise buildings are that (1) strength degradation significantly decreases the global drift capacity: whereas (2) the existence of stiffness degradation increases the global drift capacity. Details of the study and other results are summarized in the paper.

Introduction

Many studies on the capacity of various moment resisting connections and the behavior of steel moment frame buildings have been performed by the SAC project (FEMA 350, 2000) since 1994 Northridge earthquake. Based on the SAC project results, it was recommended in FEMA 355f (Foutch, 2000) that a detailed performance based design procedure should be used for performance prediction and that the global drift capacity of the steel moment frame should be calculated by the Incremental Dynamic Analysis (IDA) procedure (Luco and Cornell 2000). The effects of the hysteretic behavior of the moment connection should be included in the modeling procedure. Shi and Foutch (1997) developed a connection model for analysis of moment frames that allowed a number of different hysteresis types to be modeled in a frame analysis program. A

[1]Professor, Dept. of Engineering Technology, University of North Texas, Denton, TX 76207 (zhenhua.huang@unt.edu)
[2]Professor Emeritus, Dept. of Civil Engineering, University of Illinois at Urbana-Champaign, Urbana, IL 61801

new element (ELEMENT 10) was added in DRAIN-2DX (Prakash et al 1993), which is a well-known computer program for conducting inelastic static/dynamic structural finite element analysis. With the new element, the Nonlinear Dynamic Time History Analysis (NDTH) for moment resisting frame buildings with a variety of hysteresis models can be conducted. Yun et al. (2002) used this element to evaluate the global drift capacities of buildings with connections that fracture. Foutch and Lee (2002) evaluated the collapse potential of steel buildings with post-Northridge connections for which strength and stiffness degradation could occur but fracture could not. What is missing in prior literature is a comprehensive understanding and evaluation of the global collapse drift capacity for buildings with different features. This paper partially fills this void by collectively examining the effects of the hysteresis types. Many seismic analyses of 3-story, 9-story, and 20-story moment resisting frame buildings were conducted for this study to evaluate the effects of the hysteretic behavior of beam-to-column connections with P-delta on the global collapse drift limit. Five hysteresis models: bilinear, strength degradation, stiffness degradation, stiffness degradation + strength degradation, and pinching were evaluated.

Building Archetype and Ground Motions

Three post-Northridge building configurations designed by professionals and modified by Foutch (2000) were used for the analyses in this study. These buildings were 3-, 9- and 20-stories in height and were designed using Special Steel Moment Resisting Frames (SSMRF) to carry lateral forces. Floor plans and elevations are given in Figure 1. All of the buildings are symmetric in plan and the perimeter moment frames are designed to carry all of the seismic loads.

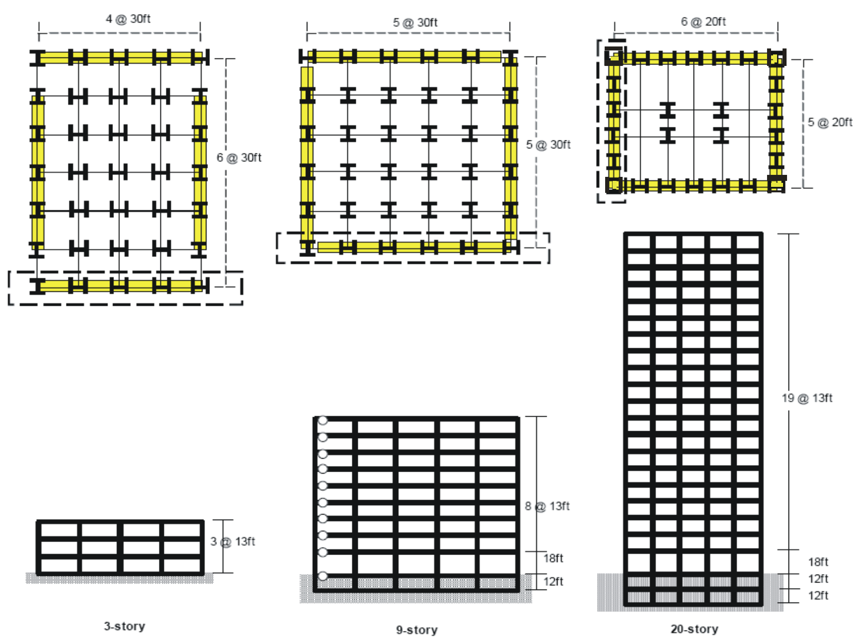

Figure 1. Plan and Elevation View of Buildings Used in this Study.

The 3-story building has no basement. Its bay widths are 30 feet, and the column heights are 13 feet. There exist three and a half bays of moment resisting frame in each of the four perimeter frames. In order to avoid the bi-axial bending, these moment resisting frames are designed to include the corner columns in only one direction. All the columns are assumed to be fixed at the base. Post-Northridge connections were used in the model at the column bases at the ground level. The 9-story building has one basement with the height of 12 feet. Each corner column also has only one moment connection to prevent bi-axial weak axis bending. The column bases are modeled as pinned-end connections, while the ground level reinforced by concrete walls restrains the lateral movement of the column at the first floor level. The 20-story building has two basement levels, each with the height of 12 feet. The basement levels are reinforced by perimeter concrete walls providing a support at each basement level. The column bases are modeled as pinned-end connections. The entire perimeter frames are designed as moment-resisting frames and the box columns are used in the corners to resist the bi-axial bending under seismic loads. The pinned connections at the ground level for the 9- and 20-story buildings were chosen by design professionals. Rigid connections for the base level columns would not significantly affect the story drifts because of the stiffening effects of the basement walls which allowed rotation of the columns but no translation at the constrained floor levels. The member properties for the buildings (Foutch, 2000) were used as the starting point for this study. The hysteresis properties were changed to represent the hysteresis behavior of both steel and reinforced concrete frames. From this point on the reader should not consider this to be a study of steel frame buildings. The material should be thought of as generic. The basic steel models were chosen as a starting point because they possess somewhat similar stiffness and strength distribution as buildings currently being constructed for each building height for a specific site in Los Angeles. So, the natural periods of vibration would be similar as well. The effects of these assumptions will be addressed and evaluated throughout the paper. RC buildings with the same heights would likely be heavier and stiffer and have similar periods as the steel frames.

Generally, the analytical models used in this study are nonlinear centerline models. The panel zone effects are neglected. This is a limitation in the study that will be addressed later in the paper. We were interested in addressing broad and general effects of hysteresis effects for a general class of moment frames. Panel zone effects would be a valid topic to investigate but this would require specific member geometry and material type to be included which is beyond the scope of this study. Beams are modeled as elastic elements that connect to the beam-to-column joint through a rotational spring. The rotational spring was placed at the end of the beam element to model inelastic behavior of the beams. Large elastic stiffness was assigned to the rotational spring to attain fully rigid connection behavior. So, the elastic beam element provides the stiffness of the frame, as it should be. For the post-yield strength, a strain-hardening rate of 0.3% was assigned after the rotational spring reaches the plastic moment capacity of the beam elements. Columns are modeled using beam-column element (ELEMENT 2) defined in the DRAIN-2DX program (Prakash et al. 1993). A bilinear interaction diagram for moment and axial force was introduced for column strength. Geometry nonlinearity was considered for the static pushover and nonlinear time history analyses. This includes the P-δ and P-Δ effects. 1.0 dead load plus 0.25 live load were applied on the frame and leaning columns for the P-delta effects. Another important point is that moment frames in each direction are the only structural elements that resist P-Δ moments whereas the gravity forces carried in all of the leaning columns produce P-Δ effects which also must be resisted by the moment frames. Viscous damping values used for the dynamic time history analysis were 4.3% for 3-story, 3.6% for 9-story, and 2.3% for the 20-story buildings. These damping values are based on studies of instrumented steel buildings that were shaken during earthquakes (Goel and Chopra, 1997). For the 3- and 9-story buildings, these damping values are fixed for the first and second modes. For the 20-story buildings, the damping value is fixed for the first and fifth modes. The natural periods of vibration for the three frame models are calculated using model analysis and given in Table 1.

Table 1. Natural Period of Building Models

	1^{st}	2^{nd}	5^{th}
3-story	1.05	0.33	--
9-story	2.70	0.97	--
20-story	3.70	1.30	0.41

Fifteen ground motions were selected from the SAC project, which include 1992 Mendocino (2), 1992 Erzincan (2), 1949 Olympia (2), 1965 Seattle (2), 1985 Valpariso (2), Deep Interpolate Simulation (2), and Shallow Interpolate Simulation (3). No hazard level needs to be considered because the incremental dynamic analysis (IDA) includes a scaling procedure.

Hysteresis Types

The connection hysteretic behavior to be studied in this project includes the effects of connection stiffness- and strength- degradation and pinching. These are modeled using a new element (ELEMENT 10) in the DRAIN-2DX program developed by Shi and Foutch (1997). Five hysteresis models for the moment connections are selected to evaluate the effects on the global drift limit in this study. They are: (1) bilinear model; (2) strength degradation model; (3) stiffness degradation model; (4) strength + stiffness degradation model; and (5) pinching model. The hysteresis models chosen for study are based on laboratory studies of steel and RC members and structures that have been conducted over the past 50 years. These include SAC 96-02 (1996), LaFave and Wight (2001), Shin and LaFave (2004) and others that are referred to below. The basic bilinear model (BL) is defined as hysteresis type 1. It has stable hysteresis loops with large energy dissipation capacity. The model consists of only two states of stress: elastic and plastic. No real member of a moment frame would behave in such a robust manner. This is merely used as a base line. The strength degradation (SD) model is defined as hysteresis type 2, which is the strength degradation version of the type 1 model. Since the exact value of degradation are unknown due to lack of experimental data, this study uses 10%, 25% and 40% for modeling. 10% degradation rate represents the behavior of current design of steel SMRF buildings with compact sections and may adequately represent special RC frames, although minor pinching and stiffness degradation may occur for RC frames; the 25% and 40% cases could represent ordinary steel frames with non-compact sections or partially restrained connections. The stiffness degradation (KD) model is defined as hysteresis type 3, which is based on the basic version of Takeda-Sozen model (Takeda, Sozen, and Nielsen 1970). The KD model represents the ideal RC member without strength degradation or pinching. The stiffness degradation plus strength degradation model (KD+SD) is defined as hysteresis type 4, which is the strength degradation version of Takeda-Sozen model. Similar to the case in previous section, 10%, 25%, and 40% strength degradation percentages are used here. The model with KD+10%SD model might be similar in nature to a special RC moment frame building. The models with KD+25%SD and

KD+40%SD might simulate the concrete moment frame structures which were built prior to the advent of the modern codes which have more stringent detailing requirements (Beres, El-Borgi, and Gergely, 1992). Pinching is another important property for a hysteresis behavior. The hysteresis loop pinching is due to the opening and closing of the cracks and/or slipping of debonded reinforcing bars in RC structures (LaFave and Wight, 2001; Shin and LaFave, 2004). For steel structures, bolt connection slippage under load reversal can cause pinching (Schneider and Teeraparbwong, 2000). The pinching model is defined as hysteresis type 5, which is the modified pinching version of the Takeda-Sozen model. In this study, the reduced force resistance level equal to 20%, 50%, and 70% of the maximum resistance are selected to evaluate the effect of pinching. Figure 2 shows the hysteretic behavior of (a) the theoretical BL model, (b) an example DRAIN-2DX BL model, (c) the theoretical SD model, (d) a measured SD behavior (Venti and Engelhardt, 1999), (e) an example DRAIN-2DX SD model, (f) the theoretical KD model, (g) a test result for an RC frame KD behavior (Bechtoula et al. 2006), (h) a DRAIN-2DX KD output, (i) the theoretical KD + SD model, (j) experimental KD+SD data (Tong et al 2005), (k) a DRAIN-2DX KD+SD model, (l) the theoretical pinching model, (m) a laboratory test pinching behavior (Elgaaly and Liu, 1997), and (n) an example of pinching model from DRAIN-2DX.

Drift Limits and Incremental Dynamic Analysis

The global drift limit is defined as the story drift at which incipient global collapse caused by P-Δ effects has been reached. This assumes that no local collapse has occurred. This may or may not represent the Collapse Limit State (CLS) proposed in many Performance Based Design (PBD) procedures because it does not account for any local collapse that may precede it. As such, the results presented herein may (at best) approximate an upper bound on the CLS. It should also be mentioned that the point of this investigation is to identify differences in the drift limit for different hysteresis types, but not absolute quantities that may be certified and included in a building code. The Incremental Dynamic Analysis (IDA) procedure developed by Luco and Cornell (1998) is employed to evaluate the global drift limits of the 3, 9, and 20-story buildings with the various hysteresis models. FEMA355f describes the IDA procedure in depth so this will not be described in detail herein. Figure 3 shows examples of IDA curves for the bilinear model compared with (a) the strength degradation (SD) models with values of 10%, 25%, and 40%, (b) the stiffness degradation (KD) model, (c) the stiffness + strength degradation (KD + SD) model, and (d) different percentage of pinching models, respectively.

The circles in the figure represent the drift limit points where the equivalent stiffness of the building (slope of the IDA curve) is less than 20% of the slope from the elastic analysis (20% criterion), this can be thought of as the point where inelastic drifts are increasing five times faster than elastic drifts for a small incremental load. The triangles represent the limit points where the slope of the IDA curve of the building is less than 10% of the slope from the elastic analysis (10% criterion). The SAC study used the 20% criterion, but in some cases this results in a very conservative estimate of the drift limit. We provide points of instability for both cases in the figures, but will focus on the results for the 20% criterion in the tables and discussion.

The IDA response is generated by subjecting the building model to an earthquake accelerogram. The amplitude of the accelerogram is incrementally increased for each time history analysis until the drift limit is reached. This is done for 15 accelerograms and the average drift limit for that case is taken as the average for the 15 runs. The maximum cutoff drift limit was arbitrarily set at 0.20. For the SAC studies the maximum drift limit was set to 0.10. This is a numerical study so no physical significance should be placed on the drift limits reaching these levels. The analytical model for drifts approaching 0.20 (or 0.10 for that matter) would not be realistic because local collapses would likely occur prior to this and/or the mathematical model would no longer be valid.

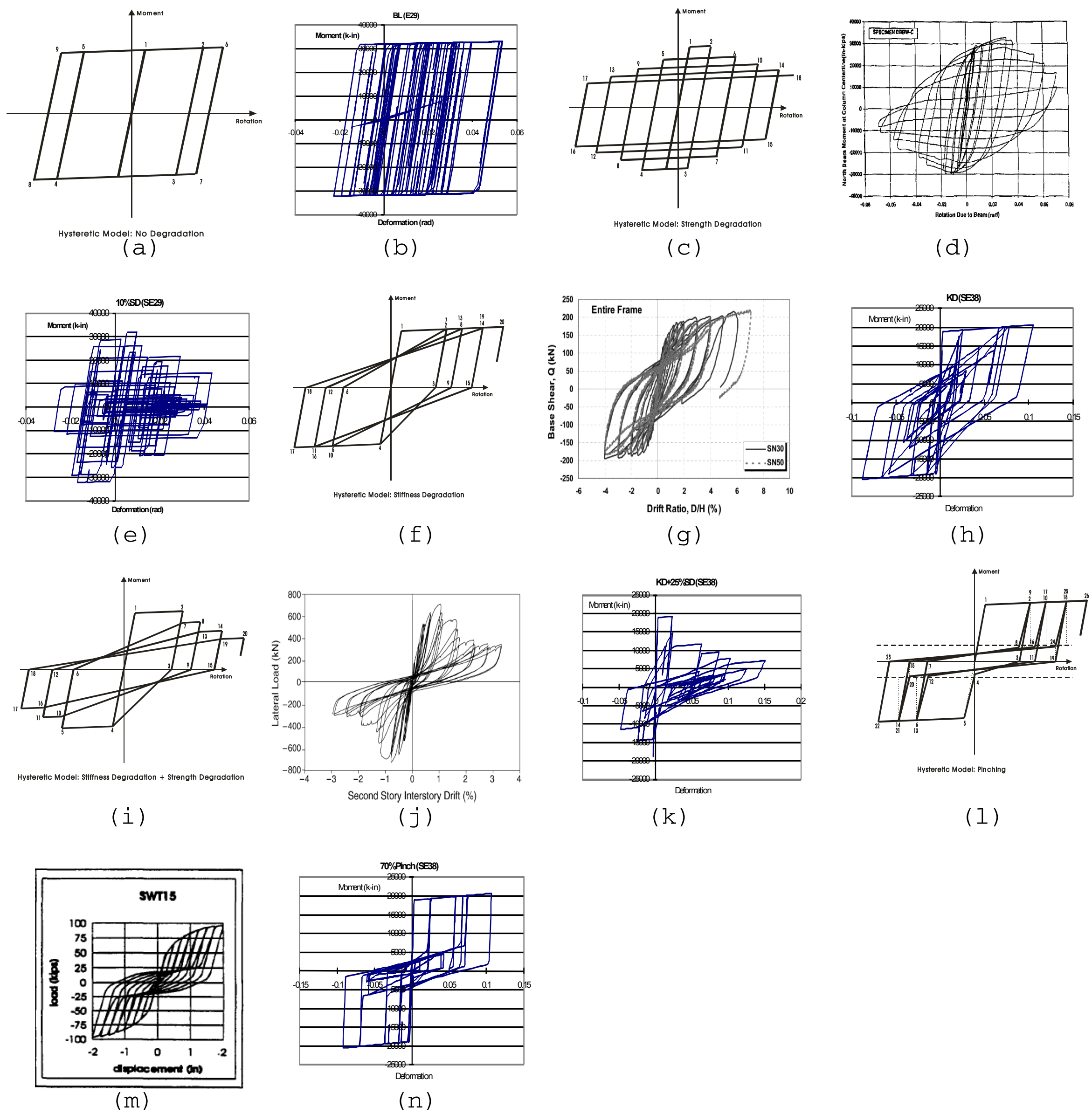

Figure 2. Hysteresis Behavior

The average global drift limit results for the 3, 9, and 20-story buildings using 20% criterion are presented in Table 2. The SAC studies suggest that the steel special moment frame building with post-Northridge connections may be able to reach a story drift approaching 0.09 before experiencing numerical global collapse. However, even these buildings may experience loss of gravity carrying capacity for parts of the frame which are not participating in the lateral load carrying system. So, a drift limit of about 0.09 is probably a practical upper bound on the drift limit for real SSMRFs structures.

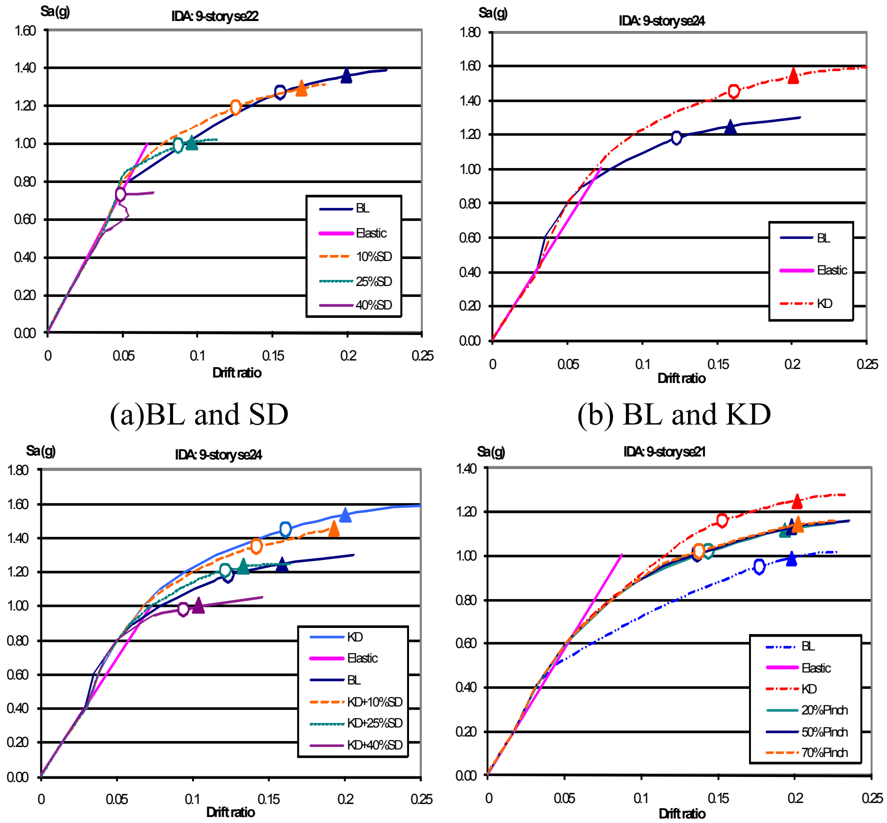

(a)BL and SD (b) BL and KD

(c)BL and KD+SD (d) BL and Pinching

Figure 3. Example IDA Curves

Table 2. Average global drift limit for different hysteresis models (20% criterion)

	BL	10% SD	25% SD	40% SD	KD	KD+10 %SD	KD+25 %SD	KD+40 %SD	20% Pinch	50% Pinch	70% Pinch
3-story	.200	.200	.200	.199	.200	.199	.198	.193	.196	.200	.200
9-story	.101	.086	.065	.059	.115	.102	.074	.061	.100	.101	.108
20-story	.096		.074				.123			.074	

Results presented above support the following observations:

1. Strength degradation, stiffness degradation, stiffness + strength degradation, and pinching have very small effect on the global drift limit for low-rise building (3-story buildings).

2. For the mid-rise (9-story) building, strength degradation significantly decreases the global drift limit. The magnitude of the decrease in drift limit depends on the magnitude of strength degradation. The magnitude of the average drift limit for 0%, 10%, 25% and 40% strength degradation using the 20% criterion are 0.101, 0.086, 0.065, and 0.059, respectively. Similar effects are found for the high-rise building (20-story).

3. For the mid-rise building (9-story), the existence of stiffness degradation increases the global drift limit by about 14% beyond the basic bilinear model if the 20% criterion is used. The results discussed above are contrary to the conventional view, i.e., a building with stiffness degradation absorbs less energy per cycle of response and therefore possesses smaller capacity. One interpretation for the contrast is that the stiffness degradation changes not only the energy absorption of the system but also the period of the system. So, the increase in the global drift limit is driven by the increase in the "effective" natural period of the model rather that the amount of energy dissipation.

4. For mid-rise buildings (9-story), the KD+SD significantly decrease the global drift limit. The magnitude of the decrease in drift limit depends on the magnitude of strength degradation; and the magnitude of the average drift limit for stiffness + 0%, 10%, 25% and 40% strength degradation are 0.101, 0.102, 0.074, and 0.061, respectively. For high-rise buildings (20-story), the effect has the same trend as that for the 9-story building.

5. Pinching behavior has a very small effect on global drift limit. The effect remains relatively constant under varying magnitudes of pinching. The limit point for the pinching model sits between those of the basic bilinear model and the stiffness degradation model. When pinching occurs, less energy is dissipated, but the effective period increases. It seems that these two effects counteract each other to some extent.

Capacity to Demand Ratio

The drift demand were analyzed in this study for the 3-story, 9-story, and 20-story buildings with basic bilinear, strength degradation, stiffness degradation, strength + stiffness degradation, and pinching hysteresis models under 15 earthquake records. The drift demand is defined as the average maximum story drift calculated for the building when subjected to an earthquake accelerogram which is scaled to represent the design spectrum for the maximum considered earthquake. Each accelerogram was scaled using a least squares procedure to match the design spectral acceleration at periods of 1.0, 2.0 and 4.0 seconds. The ratio of capacity to demand were calculated, which can be thought of as a type of factor of safety. Here, "capacity" is narrowly defined as the global drift limit as defined in this study. The relationship between demand and capacity is very important for establishing performance based design and evaluation procedures. Table 3 gives capacity/demand ratios for the 3-, 9- and 20-story buildings.

Table 3. Capacity to demand ratio for different hysteresis models (20% criterion)

	BL	**10% SD**	**25% SD**	**40% SD**	**KD**	**KD+10 %SD**	**KD+25 %SD**	**KD+40 %SD**	**20% Pinch**	**50% Pinch**	**70% Pinch**
3-story	6.4	6.3	5.8	5.5	5.8	5.7	5.3	4.4	5.8	5.7	5.6
9-story	4.1	3.4	2.6	2.3	4.5	3.9	2.7	1.8	3.9	3.9	4.1
20-story	4.9		3.4				6.1			3.2	

Based upon these results, the following observations can be made:

1. Strength degradation decreases the C/D (capacity/demand) ratio. The magnitude of the decrease depends on the magnitude of strength degradation. For example, the magnitude of the

C/D ratio for a 9-story building with 0%, 10%, 25%, and 40% strength degradation hysteresis models are 4.1, 3.4, 2.6, and 2.3, respectively.

2. The existence of stiffness degradation increases the C/D ratio for the mid-rise building.

3. Strength degradation + stiffness degradation decreases the C/D ratio. The magnitude of the decrease also depends on the magnitude of strength degradation. The magnitude of the C/D ratio for a 9-story building with stiffness degradation + 0%, 10%, 25%, and 40% strength degradation hysteresis models are 4.1, 3.9, 2.7, and 1.8, respectively.

4. Pinching behavior decreases the C/D ratio by a small amount.

Conclusion

This research conducted seismic analyses of 3, 9, and 20-story moment resisting frame buildings to evaluate the effects of the hysteretic behavior on the global drift limit due to P-delta effects. Surprisingly, only hysteresis types with strength reduction significantly affected the global drift limit of frame buildings. For other hysteresis types the global drift limit was not significantly affected. Based upon the analysis results, the following conclusions can be drawn:

1. Strength degradation and stiffness plus strength degradation have a significant effect on the calculated collapse story drift limit but little effect on story drift demand.

2. Stiffness degradation and pinching have small effect on the drift limit. This is because the stiffness decrease that occurs causes the effective fundamental period of the building to decrease which moves the building into a region of the response spectrum with lower input energy. A similar effect was also observed for hysteresis behavior where pinching occurs. Although the energy dissipated per cycle of response decreases significantly in some cases, the effective period increases so these two characteristics cancel each other.

3. The capacity/demand ratio ranges from about 4.1 to 1.8 depending on the hysteresis type. This is due in part because all of the buildings were designed for the same strength and stiffness criteria. In reality, the buildings with expected significant strength or stiffness degradation would be designed for larger seismic loads because of decreased R values. For instance, a Special Moment Frame building for a steel or RC building is 8 while the R value for an Ordinary Moment Frame of steel or RC is 4. So they would likely have smaller demand and a larger global drift limit than those used to design SMRF buildings where strength degradation and other hysteresis deterioration characteristics. It is an interesting coincidence that the ratio of the C/D ratio for the frame with the least amount of strength (or stiffness) degradation to the frame with the most amount of strength (or stiffness) is about (4.0/2.0) 2.0. The ratio of the R values for the Special Moment Frame and the Ordinary Moment Frame is (8/4) 2.0 as well.

5. All of the analyses presented in this study utilized mathematical models for which local collapses in either the gravity or lateral load carrying frames were not allowed. Local collapses may be catastrophic in their own right, or may significantly alter the lateral load resisting behavior of the building. As a result, the calculated story drift collapse limits presented herein are upper bounds at best. In fact, it is likely that these calculated drift limits will always be larger than acceptable for use as the Collapse Prevention limit state for frame structures. Not enough testing of the effects of cyclic loading on the response of gravity frames has been done for accurate modeling or for adequate design provisions to be developed for Performance Based Design.

References

Bechtoula, H., Sakashita, M., Kono, S., Watanabe, F., and Eberhard M. [2006], "Cyclic Performance of Lower Stories of Mid-Rise Reinforced Concrete Frame Buildings." ACI Structural Journal V. 103, No. 4

Beres. A., El-Borgi, S., and Gergely, P. [1992], "Behavior of Reinforced Concrete Frame Structures with Non-Ductile Details: Part 1 – Summary Findings of Full-Scale Beam-Column Joint Tests" Report NCEER-92-National Center for Earthquake Engineering Research, State University of New York at Buffalo, New York

Elgaaly, M., and Liu Y. [1999], "Analysis of Thin-Steel-Plate Shear Walls." ASCE Journal of Structural Engineering V. 123, No. 11: 1487-1496

FEMA. [2000], "Recommended seismic design criteria for new steel moment frame buildings." Rep. No. FEMA-350, SAC Joint Venture, Federal Emergency Management Agency, Washington, DC.

Foutch, D. A. [2000], "State of art report on performance prediction and evaluation of moment-resisting steel frame structures," SAC Rep. No. FEMA 355f, Federal Emergency Management Agency, Washington, D.C.

Goel R, and Chopra A. [1997]. Vibration properties of buildings determined from recorded earthquake motions. Report UCB/EERC-97/14, Earthquake Engineering Research Center, University of California, Berkeley, CA.

LaFave, J.M., and Wight, J.K. [2001], "Reinforced Concrete Wide-Beam Construction vs. Conventional Construction: Resistance to Lateral Earthquake Loads," Earthquake Spectra, V17, No.3, 479-505.

Lee, K, and Foutch D. A. [2002], "Performance Evaluation of New Steel Frame Buildings for Seismic Loads," Earthquake Engineering Structural Dynamics 31, 653-670.

Lee, K., and Foutch, D. A. [2000], "Performance prediction and evaluation of special moment frame buildings for seismic loads," SAC Background Rep. No. SAC/BD-00/25, SAC Joint Venture, Richmond, Calif.

Luco N, and Cornell C. A., [2000], "Effects of connection fractures on SMRF seismic drift demands," ASCE Journal of Structural Engineering 126:127–136.

Prakash, V., Powell, G. H., and Campbell S. [1993], DRAIN-2DX, element description and user guide, University of California Press, Berkeley.

SAC-96-02 [1996], "Connection Test Summaries", Applied Technology Council

Schneider, S.P. and Teeraparbwong, I. [2000], Bolted Flange Plate Connections, Report SAC/BD-00/05

Shi, S., and Foutch, D. A. [1997], "Evaluation of Connection Fracture and Hysteresis Type on the Seismic Response of Steel Buildings", Ph.D. Thesis, Civil Engineering Dept, University of Illinois at Urbana-Champaign, Urbana, IL.

Shin, M. and LaFave, J.M. [2004], "Seismic Performance of Reinforced Concrete Eccentric Beam-Column Connections with Floor Slabs," ACI Structural Journal, May-June, 403-412.

Takeda, T., Sozen, M. A., and Nielsen, N. N. [1970], "Reinforced Concrete Response to Simulated Earthquake", ASCE Journal of Structural Division 96: 2557-2573.

Tong, X., Hajjar, J., Schultz, A. and Shield, C. [2005], "Cyclic behavior of steel frame structures with composite reinforced concrete infill walls and partially-restrained connections," Journal of Constructional Steel Research 61:531–552.

Venti, M., and Engelhardt, M.D., (1999) "Brief Report of Steel Moment Connection Test, Specimen DBBW (Dog Bone – Bolted Web)", Internal SAC Phase 2 Report

Yun, S. and Foutch, D.A. [2002] "Modeling of Steel Moment Frames for Seismic Loads", Journal of Construction Steel Research, 58, 529-564

Yun, S., Hamburger, R. O., Cornell, C. A., and Foutch, D. A. [2002], "Seismic Performance Evaluation for Steel Moment Frames", ASCE Journal of Structural Engineering 128(4), 534–545.